1   Enhancing static-load-test identification of bridges using

2   dynamic data

3   Wen-Jun Cao [1,2]*, Chan Ghee Koh [1] and I. F. C. Smith [2,3]

4   [1]Department of Civil and Environmental Engineering, National University of Singapore,
5   117576, Singapore

6   [2] ETH Zurich, Future Cities Laboratory, Singapore-ETH Centre,

7   138602, Singapore

8   [3] Applied Computing and Mechanics Laboratory (IMAC), School of Architecture, Civil and
9   Environmental Engineering (ENAC), Swiss Federal Institute of Technology (EPFL),

10   CH-1015, Lausanne, Switzerland

11

12   **Abstract:** In situ measurements have the potential to provide valuable information

13   about the safety and the condition of bridges through implementation of system-

14   identification methodology. A significant amount of research has focused on system

15   identification using either dynamic or static measurements separately. Realizing the

16   complementary relationship between static and dynamic measurements, traditional

17   model updating methods adopt error functions to account for the residual between

18   modeling and measured values for various types of measurements. Behavioral models

19   may be inaccurate due to incomplete representation of modeling and measurement

20   uncertainties. Furthermore, the normalization of error functions may bring additional

21   uncertainty to the identification process. In this paper, an approach based on the model

22   falsification method is proposed to combine both static and dynamic measurements

23   with explicit consideration of both modeling and measurement uncertainties. A

24   measurement selection strategy is also used to help detect abnormal measurements. The

25   approach has been evaluated using a highway flyover bridge in Singapore. Dynamic

*Corresponding author.

E-mail address: caowenjun@u.nus.edu/ wenjun.cao@arch.ethz.ch (W.-J. Cao); cgkoh@nus.edu.sg (C.G Koh);

ian.smith@epfl.ch (I.F.C Smith)

measurement data include natural frequencies and mode shapes whereas static measurement data include inclinations, deflections and strains. By combining both static and dynamic measurements, this approach leads to falsification of additional model instances and obtains a more precise prediction of parameter values than approaches which interpret static measurements only.

Keywords: System identification; parameter estimation; multi-response; finite element method; static measurements; dynamic measurements

1. Introduction

Measurements obtained from sensors enable engineers to evaluate the condition of existing civil infrastructure, thus providing valuable information for asset managers. Realizing the importance of structural health monitoring, an increasing number of asset managers require instrumentation and monitoring during and after construction.

A significant amount of research has focused on the determination of unknown structural properties using data-interpretation techniques based on measurements. The most widely used technique is residual minimization, also known as model calibration. This approach aims to find the optimal parameter values that yields the best match with the corresponding measurements [1-4]. The main drawback of this method is that it either does not include uncertainties in modeling and measurements or it involves the assumption that all uncertainties are zero-mean-Gaussian-distribution along with enough measurement data to justify that such a statistical distribution is adequately reflected in the data. Such assumptions are not compatible with most applications in civil infrastructure because they do not recognize model bias and systematic uncertainty introduced by epistemic uncertainties.

Probabilistic model updating using Bayesian inference scheme dates from the 1990's. Prior knowledge of model parameters is updated by Bayesian condition probability using measurements and inspection. Instead of looking for an optimal solution, this approach estimates posterior probabilities of updated results. Many applications can be found in the literature [5-8]. Extensions of the traditional Bayesian approach include a covariance matrix to describe correlations of uncertainties for each comparison point. This method is able to provide statistical characteristics of prediction when systematic errors are adequately described. Nevertheless, risk exists when the uncertainty dependency values are incorrectly estimated, and this may result in biased posterior probability density functions (*pdf*) of the parameters [9].

In contrast to the logic of looking for the "right" parameter values, the model-falsification method follows the logic brought by Karl Popper that every scientific theory can be tested and falsified, but never logically verified [10]. A multi-model approach based on this logic was proposed by Raphael and Smith [11]. Specifically, instead of looking for the "optimal" parameter values, a set of parameter values are considered "acceptable" as long as they agree well with observations. Robert-Nicoud et al. [12] further adopted threshold boundaries to quantify the effects of modeling measurement errors. Goulet et al. [9] proposed a probabilistic extension, which is called error-domain model falsification (EDMF). This method is able to provide robust parameter identification without making assumptions on uncertainty correlations and it is most useful when dealing with systematic uncertainties. This method was evaluated for cases of existing bridges, such as the Langensand Bridge [13] and the Aarwangen Bridge [14] in Switzerland, and the Grand-Mere Bridge [15] in Canada. It has also been applied in wind engineering by Vernay et al. [16], optimal sensor placement by Papadopoulou et al. [17] and leak detection in a fresh-water supply network by Moser et al. [18].

In full-scale monitoring on existing bridges, information is usually obtained through either dynamic or static tests. Vibration monitoring data has a wide range of applications, e.g., structural identification [19-21], damage detection [22-26], upgrading assessment [27-29] etc. Many applications can be found using ambient vibration data [1, 30-31], free-vibration data [6, 32] and forced-vibration data [32, 33]. Among them, ambient vibration is the most popular due to its low cost and minimum interruption of traffic. Global characteristics such as natural frequencies, mode shapes, and modal damping directly relate to the physical properties such as stiffness, mass and damping. In static tests, bridges are loaded with heavy trucks while sensors are installed to obtain global information like deformations and inclinations and local information like strains. Pasquier et.al [14] used load-test data to reduce the uncertainty related to remaining-fatigue-life predictions. Ren et al. [34] used static displacements to update a finite element model.

However, unexpected incidents are inevitable and uncontrollable in field tests, including malfunctioning sensors, inaccessible sensor locations, poor connection between sensor and data acquisition devices, etc. Therefore, the exploitation of the measurements becomes a key issue when applying system identification.

With the presence of multiple types of measurements, the common residual-minimization approach is to find the optimal parameter values which minimize the error functions between the measured and numerical response. Sanayei et al. [35] subdivided the error functions into the static flexibility-based error function, strain-based error function and modal flexibility-based error functions to account for the residuals between modeling and measured displacements, strains and modal displacements. These error functions are combined together after they are normalized to ensure that the contribution of the objective functions is not dependent on the unit chosen. Schlune et al. [36] tested six objective functions with various normalization methods and studied

1   their effects. The main disadvantage is that each objective function influences the

2   results of identification and modeling. Besides, measurement and modeling

3   uncertainties are seldom considered. The same applies to Bayesian model updating

4   where the relative weights given to the contributions of the mode shape vectors and

5   modal frequencies in the likelihood function significantly affect the results [37].

6   The original contributions of this paper are as follows. First, we propose an

7   approach to combine both static and dynamic measurements by exploiting a user-

8   friendly data-interpretation method called model falsification. Second, we present a

9   measurement selection strategy to systematically and progressively detect abnormal

10   measurements that need to be excluded from the falsification methodology. The

11   remainder of this paper is organized as follows. Section 2 contains an introduction of

12   the system-identification method using model falsification. The proposed approach

13   which combines both static and dynamic measurements with a measurement selection

14   strategy is explained in Section 3. Section 4 covers the application to a highway flyover

15   bridge in Singapore, followed by conclusions in Section 5.

16   **2. System identification through model falsification**

17   The goal of system identification is to identify unknown system properties $\boldsymbol{\theta} =$

18    $[\theta_1, \theta_2, \theta_3, \cdots, \theta_n]$, such as geometries, material characteristics and boundary

19   conditions, using information provided by measurements $\mathbf{Y} = [y_1, y_2, y_3, \cdots, y_m]$. To

20   describe the system, behavior models $\mathbf{g}(\boldsymbol{\theta})$ are built based on initial knowledge of the

21   system and engineering judgement. Multiple model instances $\boldsymbol{\Omega}$ are generated based on

22   several combinations of system property values $\boldsymbol{\theta^k} = [\theta_1^k, \theta_2^k, \theta_3^k, \cdots, \theta_n^k]$, leading to

23   prediction $g_i(\boldsymbol{\theta^k})$ corresponding to measurement y_i for $i =$1, 2, …, m. Denote $\boldsymbol{\theta^*}$ as the

24   true parameter values, the difference between the prediction obtained $g_i(\boldsymbol{\theta^*})$ and the

25   modeling uncertainty $\mathbf{U}_{k,g_i}$ should be identical as the true value of $\mathcal{T}$. It is also equal to

1   the difference between y_i and the measurement uncertainty $\mathbf{U}_{y_i}$. See in Equation (1a).

2   By rearranging the equation, Equation (1b) is obtained by putting all uncertainties in

3   the right-hand side. The combined uncertainty is denoted as $\mathbf{U}_{c_i}$.

$$g_i(\boldsymbol{\theta}^*) \pm \boldsymbol{U}_{k,g_i} = \mathcal{T} = \; y_i \pm \boldsymbol{U}_{y_i} \tag{1a}$$

$$g_i(\boldsymbol{\theta}^*) - y_i = \boldsymbol{U}_{c_i} = \mp \boldsymbol{U}_{k,g_i} \pm \boldsymbol{U}_{y_i} \tag{1b}$$

4   Based on the error-domain-model-falsification approach (EDMF) [9,13], if the

5   difference between model predictions and measurements falls inside the threshold

6   boundaries $\{u_{low,i}, u_{high,i}\}$, the corresponding instance is considered a candidate model.

7   Otherwise, it is falsified. The threshold boundaries are defined with a *m*-dimensional

8   hyper-rectangular domain that has a probability larger than or equal to a confidence

9   level ϕ. The confidence level ϕ is adjusted using the Šídák correction to account for

10   using multiple measurements to do falsification simultaneously [9]. The adjusted

11   confidence level $\phi^{1/m}$ is calculated through Eq. (1), where $f_{\mathbf{U}_{c_i}}(u_{c_i})$ is the probability

12   density function of $\mathbf{U}_{c_i}$. ϕ is commonly set to 0.95 in civil engineering [9].

$$\phi^{1/m} = \int_{u_{low,i}}^{u_{high,i}} f_{\mathbf{U}_{c_i}}(u_{c_i}) \, d\, u_{c_i}, \forall i \in \{1, \cdots m\} \tag{2}$$

13

3. Combination of dynamic and static measurements

15   To obtain more precise predictions of parameter values, several types of

16   measurements are often needed. The mass distribution and material stiffness of bridges

17   are normally the unknown parameters in the identification process. The utilization of

18   dynamic properties (e.g., natural frequencies, mode shapes and damping ratios) is not

enough to identify these parameters because mass and stiffness can be changed by the same ratio while still providing the same eigensolutions. On the other hand, measured changes in deflections, strains and inclinations are dependent on stiffness and independent on mass distribution. Thus, static and dynamic measurements have the potential to complement each other.

In EDMF, a model instance is either accepted as a candidate model or rejected as a falsified model. Regardless of the number of measurements used, a model instance is falsified when it is not consistent with at least one measurement. The risk that potential candidate models are wrongly falsified tends to be high, especially when there is doubt related to the quality of measurements. This can further lead to the bias parameter value sets and, as a consequence, bias predictions.

Given the importance of the precision of measurements, it is essential to select good measurements to do system identification. Within the same type of measurements, Sanayei et al. [35] performed data quality analysis to assess the accuracy and reliability of the measured data. Noisiest measurements were eliminated from the measured data set based on the level of signal-to-noise ratio. Among eight load cases, 60% of displacements, 87.5% of inclinations and 65.6% of strains finally passed the data quality analysis. The average values of these three sets of tests were used in the subsequent process. Between different types of static measurements, Pasquier et al. [38] detected the erroneous measurements by carrying out sensitivity analyses of the diagnostics to single measurement removal from the data set. The diagnostics used is the number of candidate models. If the result showed a high sensitivity to a specific measured data, this data was removed from the data set.

The goal of the measurement selection strategy that is proposed in this paper is to use high-quality measurements to detect abnormal data in measurements. In this paper,

modal properties obtained through dynamic measurements are used to detect abnormal strain-gauge data.

When identifying global structural properties such as Young's modulus of concrete and beam density, modal properties are usually considered to be more useful than local static measurements such as strains. This is because strains are more sensitive to the response in their vicinity while modal characteristics are related to the global response of structure. Another reason is that the installation of strain gauges on the undersurface of concrete bridges is more complicated than the installation of accelerometers on the deck. The quality of installation will directly affect the measurement results obtained.

In this approach, it is important to make sure that the dynamic characteristics are accurate as they are used to detect abnormal static measurements and determine the confidence level in the measured data. Here, we use two methods of modal analysis and also two types of vibration data (free-vibration data due to impulsive force and ambient vibration data) to obtain the modal properties.

The logic of the proposed measurement selection strategy is consistent with the model falsification concept. A measurement is considered not abnormal until more information is introduced. The information refers to the consistency of identified parameter ranges with the more precise measurements. The process is shown in Figure 1. During the process, model falsification is performed iteratively.

The initial parameter set θ is chosen using initial knowledge (design drawings and/or on-site inspection). The modeling and measurement uncertainties U_g, U_y are quantified using sensor knowledge, previously estimated uncertainties in the modeling method (in this case, the finite element method) and engineering judgement. For example, engineering judgement is used to ensure that modeling uncertainties are at

1   least 5% and finite element models typically over-estimate rigidity. A sensitivity study

2   then needs to be carried out to select parameters according to their relative importance

3   on model predictions.

4   In system identification, model simulations are usually time consuming. For

5   traditional sampling techniques such as grid-based sampling and Latin-hypercube

6   sampling techniques, the number of simulations increases exponentially with the

7   dimensionality of the parameter sets. To save computation time, the underlying

8   relationships between system parameters and responses are approximated using

9   advanced interpolating functions within surrogate models. A typical procedure is as

10   follows:

11   (1) generate a small set of parameters and calculate their responses through finite

12   element analysis

13   (2) find the optimal surrogate models that best fit the data. Cross-validation is used

14   to check whether the surrogate models are accurate enough.

15   (3) expand the parameter set to the whole set $\mathbf{X}$, and use surrogate models to

16   predict their responses $\hat{\boldsymbol{g}}$.

17   In the second step, the measurement set is divided into static set $\mathbf{Y}_s =$

18    $[y_{s,1}, y_{s,2}, \cdots, y_{s,n_s}]$ and dynamic set $\mathbf{Y}_d = [y_{d,1}, y_{d,1}, \cdots, y_{d,n_d}]$. The corresponding

19   modeling and measurement uncertainties are $\boldsymbol{U}_{s,\hat{g}}$, $\boldsymbol{U}_{s,y}$, $\boldsymbol{U}_{d,\hat{g}}$, $\boldsymbol{U}_{d,y}$. Two model

20   falsifications are carried out to find the candidate model sets CMS_s and CMS_d using $\mathbf{Y}_s$

21   and $\mathbf{Y}_d$ separately.

22   If the identified parameter ranges $(\boldsymbol{\theta}_s, \boldsymbol{\theta}_d)$ deviate sufficiently from each other, we

23   consider that there is at least one abnormal measurement in $\mathbf{Y}_s$. Otherwise, it is assumed

24   that no abnormality is present, in which case all measurements should be used to

perform the final falsification. Notice that what constitutes a "sufficient" deviation for a measurement to be considered abnormal is a subjective judgement. In real applications, the information is embedded in measurement uncertainties [39]. It is not easy to identify this information based only on the knowledge provided by field tests. Nevertheless, with the help of error domain model falsification, the measurement uncertainties have been explicitly estimated. In this paper, we define that for each parameter θ_i, if the distance d_{θ_i} between identified parameters $\theta_{i,s}$ and $\theta_{i,d}$ is more than $\alpha = 10\%$ of the initial range R_{θ_i}, there exists abnormal static measurements. The value of α is based on engineering judgement and may vary for other applications and various confidence levels of measurements.

When measurement abnormality is detected, the measurement $y_{s,k}$ which falsifies the largest amount of model instances r_k of CMS_d is removed from $\mathbf{Y}_s$. Then, a model falsification is performed using the updated $\mathbf{Y}_s$ to obtain the new candidate model set. Several iterations may be needed to locate all the abnormal measurements. After all abnormal measurements are removed, both static and dynamic measurements are combined together $\mathbf{Y} = [\mathbf{Y}_s, \mathbf{Y}_d]$ to perform the last round of model falsification. It is possible that the candidate model set CMS_f is empty, and this may be due to several reasons including inappropriate assumptions in modeling and bad engineering judgement regarding uncertainties. At this point, an iterative process involves consideration of possible reasons and verification through activities such as new measurements and on-site inspection. A framework to address this task has been proposed by Pasquier [38] and is not explained in this paper. The final candidate model set is denoted as $CMS_f = [\boldsymbol{\theta}_f, \hat{\boldsymbol{g}}_f]$.

4. Case study

The case study involves a single-span concrete bridge for a highway flyover in Singapore, shown in Figure 2. The bridge is 32m in length, 16m in width, and is supported at each end by four bearings. The superstructure consists of four prestressed concrete beams and a 220mm-thick concrete slab. The bridge consists of 3 lanes. During the tests, Lane 1 was open to traffic while Lane 2 and Lane 3 were closed to traffic and used for testing.

4.1 Static test

In the static test, six trucks of approximately 32t each are parked on the bridge as shown in Figure 3(a). Electronic levels (Federal Electronic Level Gage Head, Model: EGH-02013W2Z) and digital readout (Mahr Amplifier model no. 832F) are installed at both ends of the bridge to measure inclinations (In1, In2). The deflections at four locations (P1~P4) are measured by prisms installed at the bottom of the beams and a laser tracker (FARO Vantage laser tracker) positioned on the road below the bridge.

Unlike other static sensors, strain gauges (TML PL-120-11-3LT, gauge length: 120mm) were installed 24 hours before the test. The installation needed pre-qualified operators on an aerial work platform and this required traffic closure below the bridge. The installation process was impaired by the poor quality of adhesive and the lack of experience of the workers. Only 8 strain gauges instead of 14 (as planned) were installed due to time constraints. The configuration of the locations of sensors is shown in Figure 3.

4.2 Free vibration test

To identify the dynamic characteristics of this highway flyover, free-vibration tests were conducted by moving trucks. Accelerometers (PCB 393B12, sensitivity: 10V/g) including eight vertical accelerometers (A1-A2, B1-B3, C1, C3-C4) and two horizontal accelerometers (A3, C2) are installed on the surface of the concrete deck

11

along both sides of the flyover; the configuration is shown in Figure 3. A1-A3 and B1-B3 are connected to DEWE-511 data acquisition system, and C1-C4 are connected to CoCo-80 handheld data acquisition system (sampling rate 1024Hz).

In order to obtain the free vibration response of the bridge, eight tests are carried out to generate the impulsive force (Table 1). 32-ton trucks move along the bridge from the east end to the west end at two speeds; the slow speed is approximately 20km/h and the fast speed is approximately 40km/h. In test 5 and test 6, a rubber speed hump (900mm x 500mm x 50mm) is installed on the surface of the designated lane to help increase the excitation.

The Fast Fourier Transform (FFT) is used on the 10s free vibration acceleration-time data to give a preliminary evaluation of the vibration properties of the bridge. The resolution of FFT is 0.1Hz. Figure 4 shows field-test photos, accelerometer signals and natural frequencies. The mean values of natural frequencies obtained are shown in Table 2.

4.3 Ambient vibration test

In the ambient vibration test, the sensor configuration is the same as that of the free vibration tests. Measurement is recorded during a period of 15 minutes when no truck is running on Lane 2 and Lane 3 while Lane 1 remains open but with only sporadic vehicles passing through. The modal properties are obtained using the stochastic subspace identification method with unweighted principle component (SSI-UPC). The stabilization diagrams are shown in Figure 5.

Four modes have been identified and the corresponding standard deviation of natural frequencies are shown in Table 3. Mode 1 is the first vertical bending mode, and Mode 2 is the torsional mode. Because all sensors are installed outside the vehicle lanes near the two sides of the bridge, and no sensor is placed on the road surface

1 between the two sides of the bridge to capture the mode shape. The mode shape

2 obtained in Mode 3 is similar to that of Mode 1. Based on the knowledge of dynamic

3 properties of a simply supported beam, it is easy to infer that Mode 3 is a lateral bending

4 mode, i.e. the bridge is bending in the horizontal direction. Mode 4 is the second vertical

5 bending. These measurement results are consistent with the numerical results obtained

6 by finite element analysis.

7 **4.4 System identification using both static and dynamic measurements**

8   The flyover is modeled in ANSYS [40] using a 3D solid element (element type

9 "SOLID 185") shown in Figure 6. The mesh size is 0.2m. Boundary conditions are

10 modeled using linear springs. Parameters to be identified include Young's modulus of

11 concrete (E), concrete density (D), logarithm of bending stiffness of bearings (LogB),

12 logarithm of vertical stiffness of bearings (LogV) and logarithm of longitudinal

13 stiffness of bearings (LogL). In this case study, the design drawings we received are

14 not the as-built reality and on-site measurement of real geometric dimensions was not

15 allowed by the bridge owner due to time constraints related to the bridge closure. As a

16 result, the concrete density (D) is in fact an "equivalent density" accounting for the

17 geometric discrepancies. The logarithmic values of bearing stiffness are used because

18 the dynamic characteristics of the bridge are influenced by the orders of magnitude,

19 rather than the precise bearing stiffness values, based on parametric study of the finite

20 element model.

21   The initial ranges of all parameter values are defined based on engineering

22 experience and information obtained from drawings, as shown in Table 4. Note that the

23 four girders are considered to have the same boundary conditions.

24   A sensitivity analysis is conducted to evaluate the relative importance of

25 parameters with respect to responses. Analysis of variance (ANOVA) is used [41] by

13

calculating the coefficient of determination (R^2) for the quadratic correlation between them. When R^2 is smaller than 5%, the influence of parameter to the response can be neglected. The results in Figure 7 show that the influences of material properties (E and D) are large on the dynamic response, while E also influences greatly the static responses. Among the bearing parameters, LogV is influential on deflections (P1~P4) and inclinations (In1~In2). Nearly all static responses are sensitive to LogB. LogL is the least influential parameter and is neglected by the 5% R^2 threshold. Hence, all parameters except LogL are selected to perform system identification.

Following the procedure of generating surrogate models, first, 1000 model instances generated by the Latin-hypercube sampling technique [42] are calculated using finite element analysis. Then, surrogate models are built based on Gaussian process, resulting in $50^4 = 6,250,000$ samples (50 discrete values for every parameter).

In this study, uncertainties are described using uniform distributions and are generally expressed as ratios (in percentage) of the parameter values. Uncertainties are calculated as the product of the ratio and the corresponding predicted or measured values. Sensor accuracies are taken from the respective product specifications. In dynamic measurements, the uncertainty related to modal analysis is considered by taking into account the results obtained by free vibrations and ambient vibrations. Other uncertainty values are taken in according to [13,38,43]. The details are shown in Table 5 and Table 6.

Modeling uncertainties are also introduced by adopting surrogate models. To evaluate how accurately a surrogate model is able to predict values for unseen data, generalization error was calculated using 4-fold cross validation (k=4) in this case study. The training data including parameters $\boldsymbol{\theta}_{tr}$ and responses $\mathbf{Y}_{tr}$ are randomly divided into 4 subsets. Each data subset is then used as a test set S_j^{test} including n pairs of

parameters $\boldsymbol{\theta}_j^{test}$ and responses $\boldsymbol{y}_j^{test}$, with the remaining data acting as a training set $S_j^{train} = \{\boldsymbol{\theta}_j^{train}, \boldsymbol{y}_j^{train}\}$. Surrogate models $\widehat{\boldsymbol{g}}$ are generated by the training set and are used to predict the response of test data $\widehat{\boldsymbol{g}}(\boldsymbol{\theta}_j^{test})$. The usual average test set error $\hat{\mu}_i$ and generalization error $\hat{\mu}$ are calculated following (3) and (4). The calculated surrogate model uncertainties are shown in Table 7.

$$\hat{\mu}_i = \frac{1}{n}\sum_{i \in S_j^{test}} \left| \widehat{\boldsymbol{g}}(\boldsymbol{\theta}_j^{test}) - \boldsymbol{y}_j^{test} \right| / \boldsymbol{y}_j^{test} \qquad (3)$$

$$\hat{\mu} = \frac{1}{k}\sum_{i=1}^{k} \hat{\mu}_i \qquad (4)$$

4.5 Results and Discussion

First, all available static measurements and dynamic measurements are used to perform identification. For the dynamic part, the modal assurance criterion is calculated to ensure the same mode is compared. Then, the natural frequencies are used to perform model falsification. Candidate model sets (CMS_s^k and CMS_d^k) are obtained using static and dynamic measurements separately in the kth iteration. The identified parameter values are shown in Figure 8. The identified E values vary from 39,800 MPa to 42,000 MPa in CMS_s^1 and from 26,740 to 29,900 MPa in CMS_d^1. The distance d_E^1 between the two ranges is 9,900 MPa, which is 45% of the whole range of R_E. This already exceeds the threshold $\alpha = 10\%$ implying the existence of abnormal measurements. Then, we investigated the falsification capability of each static measurement and found that S8 falsifies the biggest portion of CMS_d^1. Thus S8 is removed from the measurement set.

A new model falsification is carried out based on the new measurement sets. The identified E values range from 34,400 MPa to 42,000 MPa in CMS_s^2. The distance d_E^2 between two ranges is 4,500 MPa, which is 20% of the whole range R_E. This value also

15

1   exceeds α. Following the same procedure of the previous iteration, S2 is removed from

2   the measurement set.

3   In the following iterations, S7, S3, S4, S6 are removed from the static

4   measurement set in a sequence. The quality of these sensor signals was likely

5   compromised by the installation process due to inexperienced workers as mentioned

6   earlier.

7   In the last iteration, the ranges of $\boldsymbol{\theta}_{E,s}$ and $\boldsymbol{\theta}_{E,d}$ overlap (as shown in Figure 9).

8   The identified sets of parameter E in each iteration is shown in Figure 9. The dots

9   indicate the identified parameter values using static measurements $\theta_{E,s}$ and the small

10   circles represent the ones obtained using dynamic measurements $\theta_{E,d}$. After the last

11   iteration, the remaining static measurements are P1, P2, P3, P4, S1, S5, In1, In2,

12   Following our methodology, all selected static and dynamic measurements should

13   be combined together to determine the candidate models. To study the effects of using

14   both types of data, we create three different scenarios. In Scenario I, the information

15   provided by dynamic measurements are used, which falsify 6,210,000 model instances

16   and lead to 40,000 candidate model instances. In Scenario II, static measurements (after

17   removing abnormal measurements) are used and 6,138,751 model instances are

18   falsified leading to 111,249 candidate model instances. In Scenario III, both static and

19   dynamic measurements are used, which falsify the largest number (6,248,881) of model

20   instances leading to 1,119 candidate model instances. The results show that the

21   falsification capability is greatly enhanced by using both static and dynamic

22   measurements. 98.99% candidate model instance in Scenario II are falsified by

23   introducing dynamic measurements.

24   The identified range of parameters by using both measurements is shown in Figure

25   10. The vertical axes represent parameter values and predictions of static data and

dynamic data. Each grey line represents a candidate model instance. The red dashed lines represent the threshold boundaries calculated for each response. Arrows represent the corresponding measured values.

5. Conclusions

In this paper, an approach based on model falsification is proposed to combine both static and dynamic measurements with explicit representation of both modeling and measurement uncertainties. A measurement selection strategy is also presented to detect abnormal measurements that need to be excluded from the falsification framework.

1. This approach has been successfully applied to a highway flyover bridge in Singapore. The measurement selection strategy eliminates six abnormal strain data in a systematic and progressive way. The identification results have been improved significantly by using both static and dynamic measurements. Specifically, in this case study, dynamic measurements help further falsify 98.99% of the candidate models obtained using only static measurements.

2. The proposed measurement selection strategy would help asset managers to locate possible abnormal sensors and make adjustments to sensor installation if needed. Not being limited to the application presented in the case study (using dynamic measurements to detect abnormal strain data), this strategy also applies to subsets of experiment data, i.e. to use high-quality measurement data to detect abnormal low-quality measurement data.

3. The proposed framework incorporates the use of surrogate models and associated uncertainty quantification. It enables efficient execution of the identification process. In the case study, only 1,000 FEM analyses are carried out to support 6,250,000 simulations using surrogate models.

As a multiple-model approach, the output of the identification process is a set of parameter ranges. They are considered acceptable due to the presence of uncertainties. Future work will focus on determining efficient ways to employ the candidate models for prediction.

Acknowledgements

References

1. Araujo IG, Maldonado E, Cho GC. Ambient vibration testing and updating of the finite element model of a simply supported beam bridge. *Frontiers of Architecture and Civil Engineering in China*. 2011;5(3):344.

2. Wan HP, Ren WX. A residual-based Gaussian process model framework for finite element model updating. *Computers & Structures*. 2015;156:149-59.

3. Jafarkhani R, Masri SF. Finite element model updating using evolutionary strategy for damage detection. *Computer-Aided Civil and Infrastructure Engineering*. 2011;26(3):207-24.

4. Okasha NM, Frangopol DM, Orcesi AD. Automated finite element updating using strain data for the lifetime reliability assessment of bridges. *Reliability Engineering & System Safety*. 2012;99:139-50.

5. Yuen KV, Beck JL, Katafygiotis LS. Efficient model updating and health monitoring methodology using incomplete modal data without mode matching.

Structural Control and Health Monitoring. 2006;13(1):91-107.

6. Cheung SH, Beck JL. Calculation of posterior probabilities for Bayesian model class assessment and averaging from posterior samples based on dynamic system data. *Computer-Aided Civil and Infrastructure Engineering*. 2010;25(5):304-21.

7. Beck JL, Katafygiotis LS. Updating models and their uncertainties. I: Bayesian statistical framework. *Journal of Engineering Mechanics*. 1998;124(4):455-61.

8. Goller B, Schueller GI. Investigation of model uncertainties in Bayesian structural model updating. *Journal of sound and vibration*. 2011;330(25):6122-36.

9. Goulet JA, Smith IFC. Structural identification with systematic errors and unknown uncertainty dependencies. *Computers & structures*. 2013;128:251-8.

10. Popper K. *The logic of scientific discovery*. Routledge; 2005.

11. Raphael B, Smith IFC. Finding the right model for bridge diagnosis. *In Artificial intelligence in structural engineering* 1998 (pp. 308-319). Springer, Berlin, Heidelberg.

12. Robert-Nicoud Y, Raphael B, Smith IFC. System identification through model composition and stochastic search. *Journal of computing in civil engineering*. 2005;19(3):239-47.

13. Goulet JA, Kripakaran P, Smith IFC. Multimodel structural performance monitoring. *Journal of structural engineering*. 2010;136(10):1309-18.

14. Pasquier R, Goulet JA, Acevedo C, Smith IFC. Improving fatigue evaluations of structures using in-service behavior measurement data. *Journal of Bridge Engineering*. 2014;19(11):04014045.

15. Goulet JA, Texier M, Michel C, Smith IFC, Chouinard L. Quantifying the effects of modeling simplifications for structural identification of bridges. *Journal of Bridge Engineering*. 2013;19(1):59-71.

16. Vernay DG, Raphael B, Smith IFC. Improving simulation predictions of wind around buildings using measurements through system identification techniques. *Building and Environment*. 2015;94:620-31.

17. Papadopoulou M, Raphael B, Smith IFC, Sekhar C. Optimal sensor placement for time-dependent systems: Application to wind studies around buildings. *Journal of Computing in Civil Engineering*. 2015;30(2):04015024.

18. Moser G, Paal SG, Smith IFC. Leak Detection of Water Supply Networks Using Error-Domain Model Falsification. *Journal of Computing in Civil*

Engineering. 2017;32(2):04017077.

19. Mottershead JE, Friswell MI. Model updating in structural dynamics: a survey. *Journal of sound and vibration.* 1993;167(2):347-75.

20. Wan HP, Mao Z, Todd MD, Ren WX. Analytical uncertainty quantification for modal frequencies with structural parameter uncertainty using a Gaussian process metamodel. *Engineering Structures.* 2014;75:577-89.

21. Koh CG, See LM, Balendra T. Estimation of structural parameters in time domain: a substructure approach. *Earthquake Engineering & Structural Dynamics.* 1991;20(8):787-801.

22. Salawu OS. Detection of structural damage through changes in frequency: a review . *Engineering Structures.*1997;19:718–23.

23. Teughels A, De Roeck G. Structural damage identification of the highway bridge Z24 by FE model updating. *Journal of Sound and Vibration.* 2004;278(3):589-610.

24. Simoen E, De Roeck G, Lombaert G. Dealing with uncertainty in model updating for damage assessment: A review. *Mechanical Systems and Signal Processing.* 2015;56:123-49.

25. Xu ZD, Wu Z. Energy Damage detection strategy based on acceleration responses for long-span bridge structures, *Engineering Structures,* 2007, 29(4):609-617.

26. Xu ZD, Liu M, Wu Z, Zeng, X. Energy damage detection strategy based on strain responses for long-span bridge structures, *Journal of Bridge Engineering,* ASCE, 2011, 16(5):162-171.

27. Brownjohn JM, Moyo P, Omenzetter P, Lu Y. Assessment of highway bridge upgrading by dynamic testing and finite-element model updating. *Journal of Bridge Engineering.* 2003;8(3):162-72.

28. Zárate BA, Caicedo JM. Finite element model updating: Multiple alternatives. *Engineering Structures* 2008;30:3724–30.

29. Ren WX, Chen HB. Finite element model updating in structural dynamics by using the response surface method. *Engineering Structures* 2010;32.

30. Gentile C, Gallino N. Ambient vibration testing and structural evaluation of an historic suspension footbridge. *Advances in Engineering Software.* 2008;39(4):356-66.

31. Liu C, DeWolf JT, Kim JH. Development of a baseline for structural health monitoring for a curved post-tensioned concrete box–girder bridge. *Engineering*

Structures. 2009;31(12):3107-15.

32. Ni YC, Zhang FL, Lam HF. Series of full-scale field vibration tests and Bayesian modal identification of a pedestrian bridge. *Journal of Bridge Engineering*. 2016;21(8):C4016002.

33. De Sortis A, Antonacci E, Vestroni F. Dynamic identification of a masonry building using forced vibration tests. *Engineering Structures*. 2005;27(2):155–65.

34. Ren WX, Fang SE, Deng MY. Response surface–based finite-element-model updating using structural static responses. *Journal of Engineering Mechanics*. 2010;137(4):248-57.

35. Sanayei M, Khaloo A, Gul M, Catbas FN. Automated finite element model updating of a scale bridge model using measured static and modal test data. *Engineering Structures*. 2015;102:66-79.

36. Schlune H, Plos M, Gylltoft K. Improved bridge evaluation through finite element model updating using static and dynamic measurements. *Engineering structures*. 2009;31(7):1477-85.

37. Goller B, Beck JL, Schueller GI. Evidence-based identification of weighting factors in Bayesian model updating using modal data. *Journal of Engineering Mechanics*. 2011;138(5):430-40.

38. Pasquier R, Smith IFC. Iterative structural identification framework for evaluation of existing structures. *Engineering structures*. 2016;106:179-94.

39. Aggarwal CC. *Outlier analysis. In Data mining* 2015 (pp. 237-263). Springer, Cham.

40. ANSYS, IC. *User's manual 17.0. Pennsylvania: ANSYS* 2016.

41. Saltelli A, Ratto M, Andres T, Campolongo F, Cariboni J, Gatelli D, Saisana M, Tarantola S. *Global sensitivity analysis: the primer*. John Wiley & Sons; 2008.

42. McKay M. Latin hypercube sampling as a tool in uncertainty analysis of computer models . *Proceedings of the 24th conference on winter simulation* 1992; 129815: 557–564.

43. Proverbio M, Costa A, Smith IFC. Adaptive Sampling Methodology for Structural Identification Using Radial-Basis Functions. *Journal of Computing in Civil Engineering*. 2018;32(3):04018008.

1 **Table Captions**

2 ➢ Table 1: Details of dynamic tests

3 ➢ Table 2: Identified natural frequencies using free vibrations

4 ➢ Table 3: Operational modal analysis results

5 ➢ Table 4: Parameter initial ranges

6 ➢ Table 5: Uncertainty sources of static measurements

7 ➢ Table 6: Uncertainty sources of dynamic measurements

8 ➢ Table 7: Surrogate model uncertainties

9

10

1 **Figure Captions**

2 ➢ Figure 1: Flowchart of system identification using both static and dynamic

3 measurements

4 ➢ Figure 2: Photos of the highway flyover (image credit: FCL-CCI)

5 ➢ Figure 3: Sensor configuration and truck configuration in the static test:

6 (a) top view; (b) bottom view

7 ➢ Figure 4: Dynamic test 2 (a) field test photo, (b) signal recorded by C1, (c) FFT

8 result; Dynamic test 5 (d) field test photo, (e) signal recorded by A1, (f) FFT result.

9 ➢ Figure 5: Stabilization diagrams (SSI-UPC)

10 ➢ Figure 6: Finite element model of the bridge

11 ➢ Figure 7: Parameter sensitivity results

12 ➢ Figure 8: Parameter values of CMS_s^1 and CMS_d^1. Each vertical axis represents a

13 parameter.

14 ➢ Figure 9 : Identified E values by CMS_s and CMS_d during each iteration

15 ➢ Figure 10: Identified parameter sets using both static and dynamic measurements

16

1

Table 1: Details of dynamic tests

Test No.	1	2	3	4	5	6	7	8
Vehicle numbers	1	1	1	2	1	1	2	1
Speed	slow	slow	fast	slow	slow	slow	slow	fast
Lane	2	3	2	3	2	3	2	3
Hump					yes	yes		

2
3
4
5

Table 2: Identified natural frequencies using free vibrations

	Mode 1	Mode 2	Mode 3	Mode 4
Natural frequency (Hz)	4.0	6.1	10.1	14.8
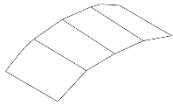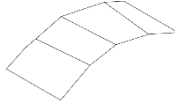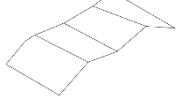
6
7
8
9

Table 3: Operational modal analysis results

	Mode 1	Mode 2	Mode 3	Mode 4
Mode Shape				
Frequency	3.982Hz	6.128Hz	9.929Hz	14.567Hz
Std. Frequency	0.012Hz	0.011Hz	0.008Hz	0.002Hz

10
11

1 Table 4: Parameter initial ranges

Parameter	Description	Lower bound	Upper bound	Sensitivity analysis results
E (MPa)	Young's modulus of concrete	20,000	40,000	keep
D (kg/m^3)	Density of the bridge	1800	3000	keep
LogB (Nmm/rad)	log of the bending stiffness of bearing	9	13	keep
LogV (N/mm)	log of the vertical stiffness of bearing	8	11	keep
LogL (N/mm)	log of the longitudinal stiffness of bearing	9	11	delete

2

3

1 Table 5: Uncertainty sources of static measurements

Uncertainty source		Displacement (P1~P4)		Rotations (In1~In2)		Strains (S1~S8)	
		Min	Max	Min	Max	Min	Max
Modeling uncertainties	Model simplifications and FE method (%)	-5	13	-5	13	-5	13
	Mesh refinement (%)	-1	1	-1	1	-1	1
	Spatial variability (%)	-	-	-	-	-5	5
	Additional uncertainty (%)	-1	1	-1	1	-1	1
	Surrogate model uncertainty (%)	Shown in Table 7					
Measurement uncertainties	Sensor accuracy	-0.05mm	0.05mm	-1μrad	1μrad	-2$\mu\epsilon$	2$\mu\epsilon$
	Repeatability	-0.15mm	0.15mm	-4μrad	4μrad	-4$\mu\epsilon$	4$\mu\epsilon$
	Sensor orientation (%)	-	-	-	-	0	6
	Sensor installation (%)	-	-	-5	5	0	5

2

3

1 Table 6: Uncertainty sources of dynamic measurements

Uncertainty source		Measured frequency (Hz)			
		4.0	6.1	10.057	14.732
		f_1	f_2	f_3	f_4
Modeling uncertainties	Model simplifications and FE method (%)	[-8, 5]	[-8, 5]	[-8, 5]	[-8, 5]
	Mesh refinement (%)	[0, 2]	[0, 2]	[0, 2]	[0, 2]
	Additional uncertainty (%)	[-1, 1]	[-1, 1]	[-1, 1]	[-1, 1]
	Surrogate model uncertainty	Shown in Table 7			
Measurement uncertainties	Modal analysis results (Hz)	[-0.1, 0.1]	[-0.1, 0.1]	[-0.144, 0.144]	[-0.169, 0.169]
	Additional uncertainty (%)	[-1, 1]	[-1, 1]	[-1, 1]	[-1, 1]

2

3

1

Table 7: Surrogate model uncertainties

	f_1	f_2	f_3	f_4
Surrogate model uncertainties Min/ Max (%)	∓0.012	∓0.011	∓0.012	∓0.026
	P1	P2	P3	P4
	∓0.3	∓0.65	∓0.25	∓0.33
	S1	S2	S3	S4
	∓0.26	∓0.24	∓0.25	∓0.22
	S5	S6	S7	S8
	∓0.22	∓0.22	∓0.24	∓0.3
	In1	In2		
	∓0.33	∓0.59		

2

3
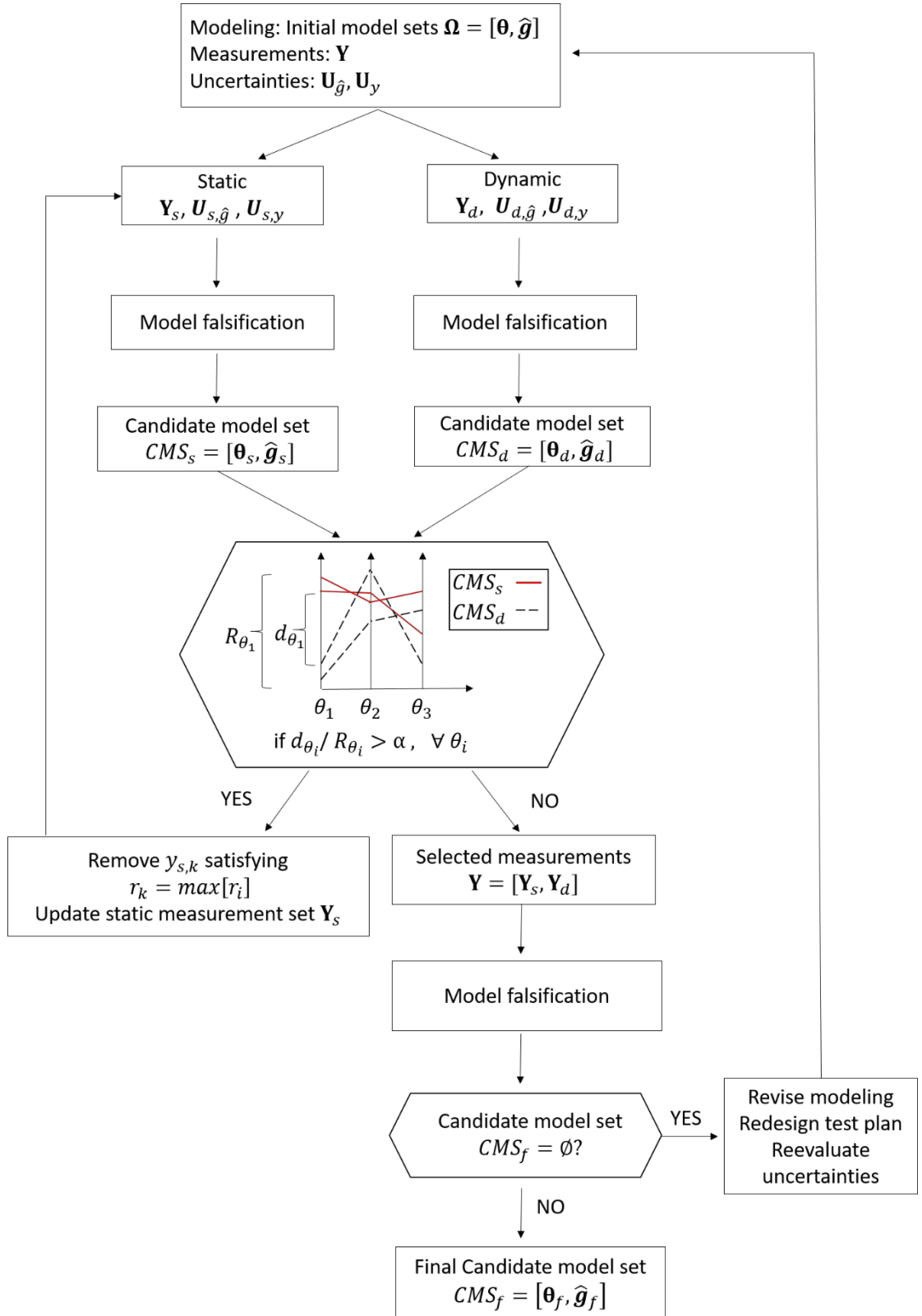
1

2   Figure 1: Flowchart of system identification using both static and dynamic

3   measurements

Figure 2: Photos of the highway flyover (image credit: FCL-CCI)

(a)   (b)
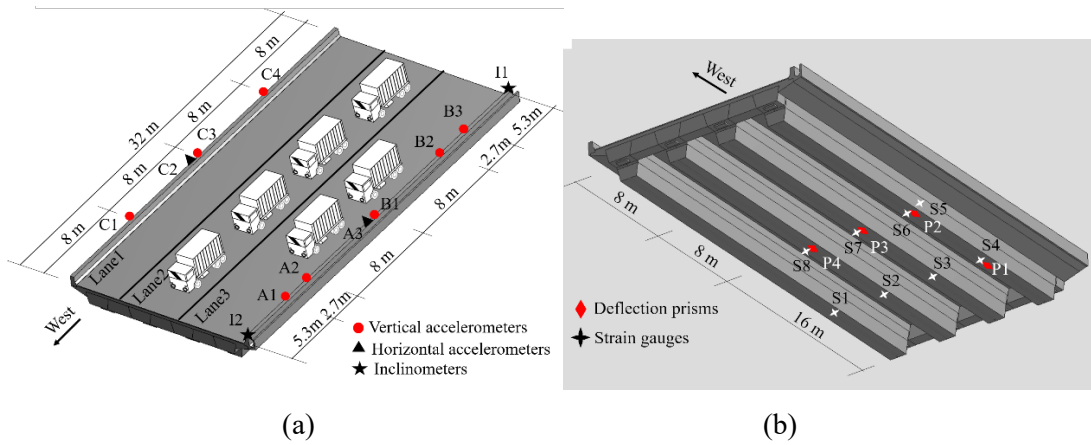
Figure 3: Sensor configuration and truck configuration in the static test:

(a) top view; (b) bottom view

(a)

(d)
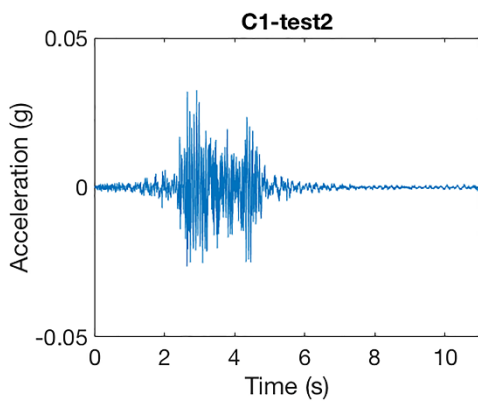
(b)
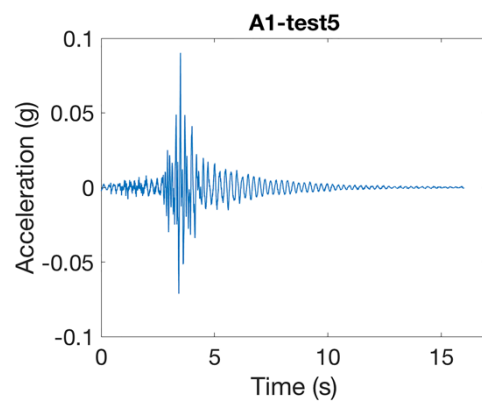
(e)
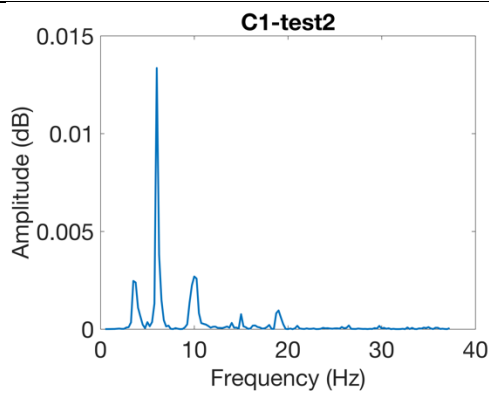
(c)
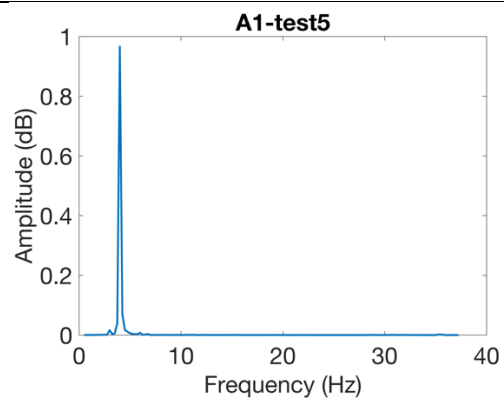
(f)

Figure 4: Dynamic test 2: (a) field test photo, (b) signal recorded by C1, (c) FFT result; Dynamic test 5: (d) field test photo, (e) signal recorded by A1, (f) FFT result.

1
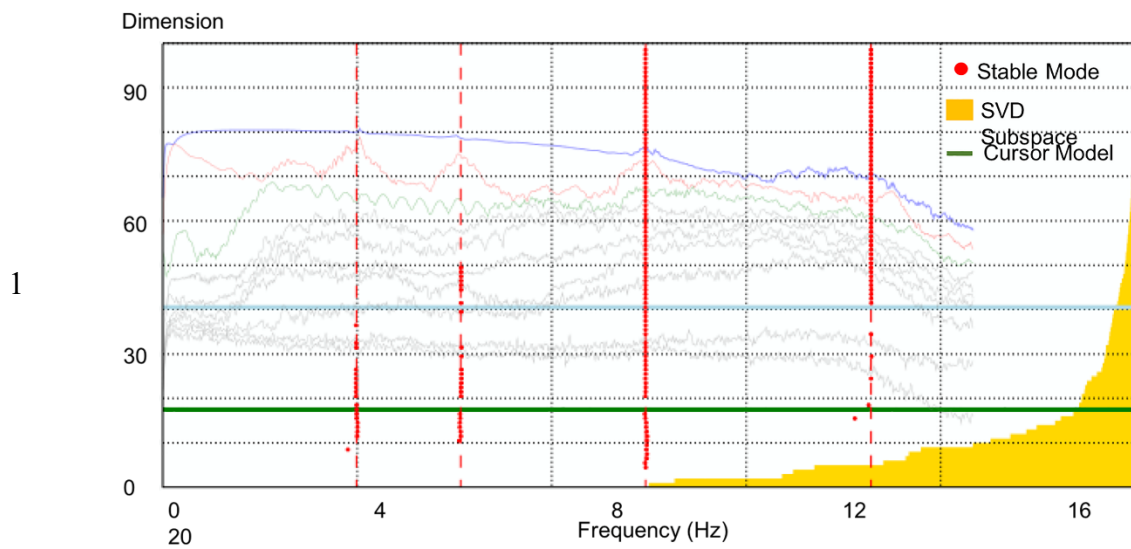
2 Figure 5: Stabilization diagrams (SSI-UPC)
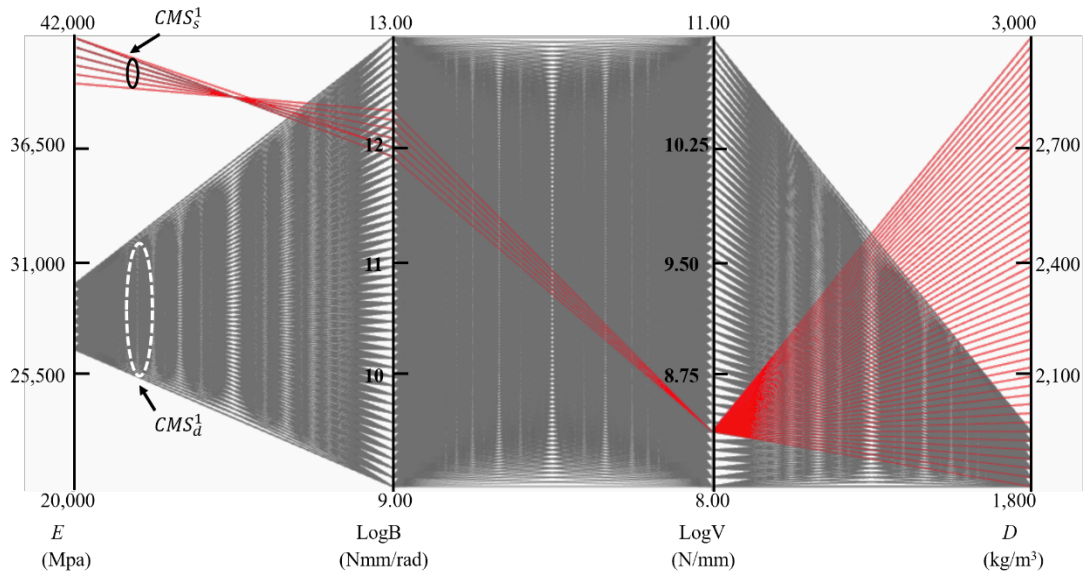
3
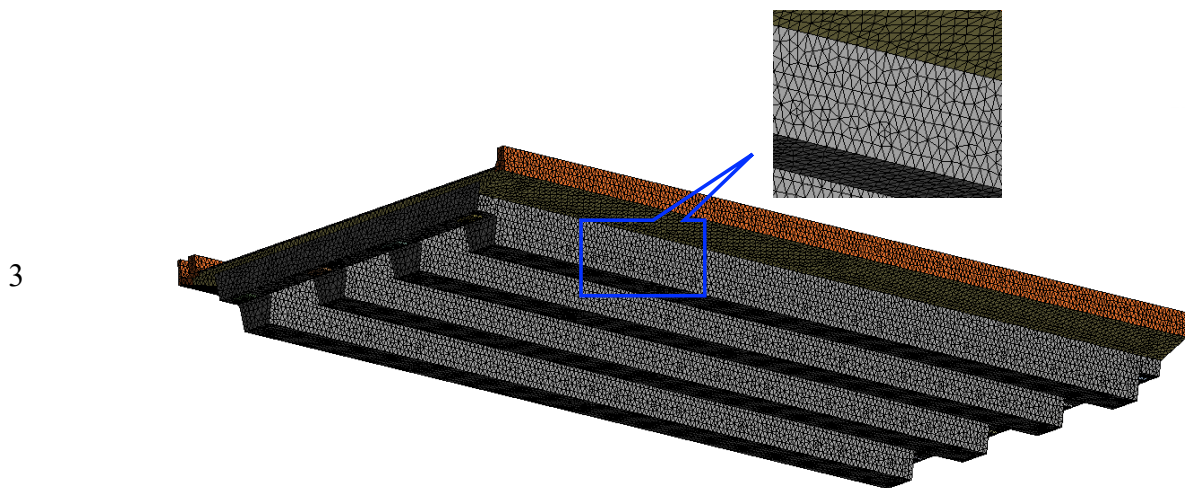
4 Figure 6: Finite element model of the bridge

5
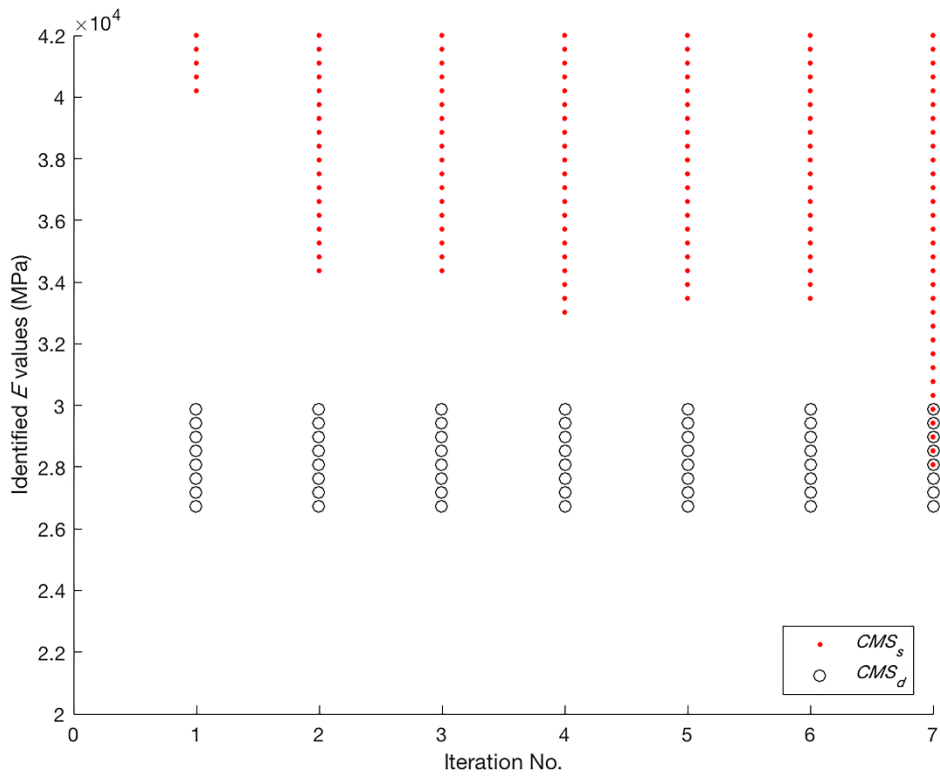
1

2 Figure 7: Parameter sensitivity results

3

1
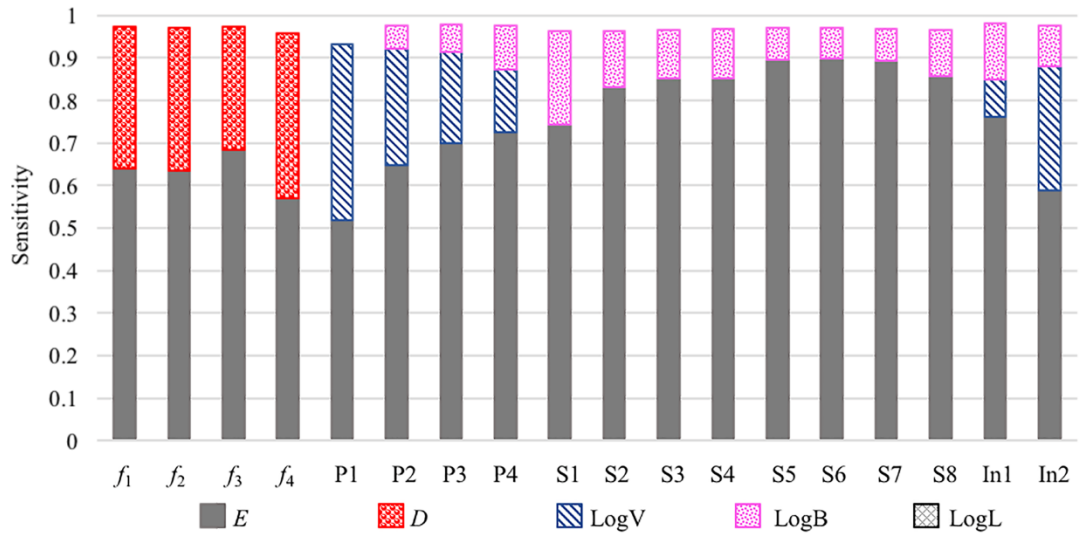
3   Figure 8: Parameter values of CMS_s^1 and CMS_d^1. Each vertical axis represents a

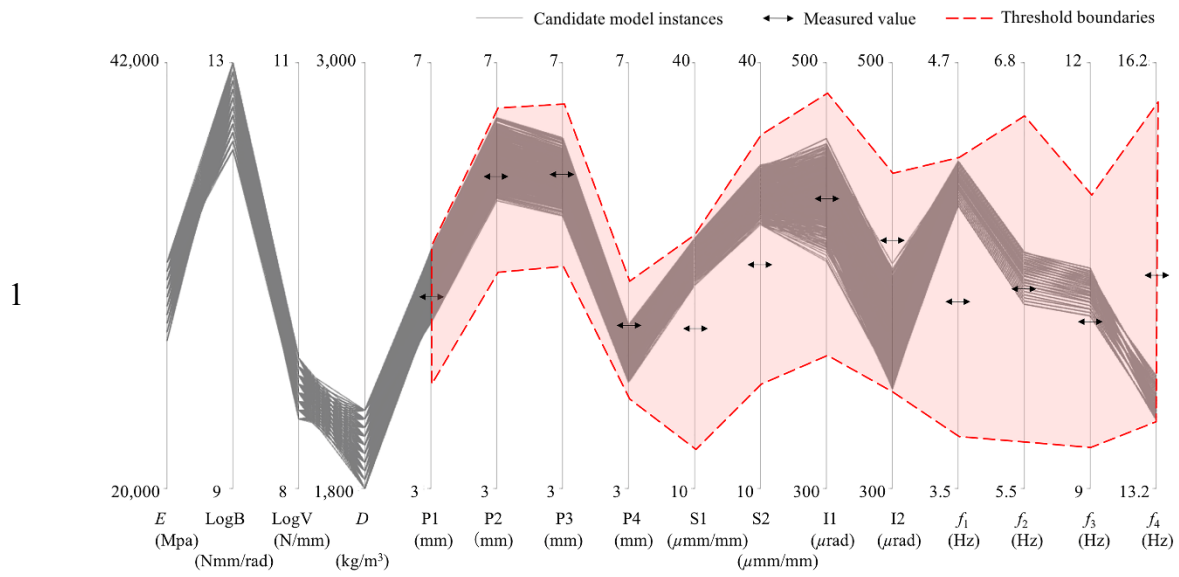4   parameter.

5

6

7   Figure 9: Identified E values by CMS_s and CMS_d during each iteration

1

Figure 10: Identified parameter sets using both static and dynamic measurements